IEEE/CSC & ESAS EUROPEAN SUPERCONDUCTIVITY NEWS FORUM, No. 22, October/November 2012.
The published version of this preprint appeared in IEEE Transactions on Applied Superconductivity 23, 6601005 (June 2013).

Mechanism of self-epitaxy in buffer layer for coated conductors

Takahiro Taneda, Masateru Yoshizumi, Takahiko Takahashi, Reiji Kuriki, Takaomi Shinozaki, Teruo Izumi, Yuh Shiohara, Yasuhiro Iijima, Takashi Saitoh, Ryuji Yoshida, Takeharu Kato, Tsukasa Hirayama, and Takanobu Kiss

***Abstract*—To elucidate the self-epitaxy mechanism of pulsed-laser deposition (PLD)-CeO_2, a hypothetical relationship with the substrate was derived based on the ion-beam-assisted deposition (IBAD) layer-processing method: the smaller the misorientation angle, the larger the crystallite size. In-plane misorientation angle dependences of crystallite sizes of IBAD-MgO and $LaMnO_3$ as substrates for CeO_2 deposition, obtained using X-ray diffraction (XRD) and transmission electron microscopy (TEM), indicated that the hypothesis was plausible. This relationship is regarded as a prerequisite for self-epitaxy because large crystallites with small strains would be energetically favorable when CeO_2 particles crystallize on them. Eventually, they will grow to dominant grains, which is a possible self-epitaxy mechanism.**

***Index Terms*—CeO_2 buffer layer, IBAD, in-plane misorientation angle, Self-epitaxy, YBCO coated conductor**

I. Introduction

SELF-EPITAXY HAS been observed in several film deposition processes. In this process, the distribution of in-plane misorientation angles, $\Delta\phi$, of the crystals of a deposited material decreases with increasing film thickness.

This phenomenon was discovered by Muroga *et al*. in 2002 [1]. They reported that CeO_2 showed excellent self-epitaxy efficiency on $Gd_2Zr_2O_7$ (GZO) substrates deposited using ion-beam-assisted deposition (IBAD), in terms of the short time needed to reach the target $\Delta\phi$ value, which is critically important for producing coated conductors with high superconducting properties at reasonable cost. Since then, self-epitaxy has been used in industrial buffer layer fabrication processes for coated conductors. Our group has been studying on the mechanism of self-epitaxy; however, it is not yet fully understood [2]-[4]. It is necessary to elucidate the mechanism so that buffer layers with smaller $\Delta\phi$ values can be produced at a higher throughput.

Manuscript received October 6, 2012. This work was supported in part by the New Energy and Industrial Technology Development Organization (NEDO) as a Materials and Power Application of Coated Conductors (M-PACC) Project.

T. Taneda, M. Yoshizumi, T. Takahashi, R. Kuriki, T. Shinozaki, T. Izumi, and Y. Shiohara are with Superconductivity Research Laboratory (SRL), International Superconductivity Technology Center (ISTEC), Koto-ku, Tokyo 135-0062 Japan (phone: +81-3-3536-5711; fax: +81-3-3536-8311; e-mail: taneda-takahiro@istec.or.jp).

Y. Iijima and T. Saitoh are with Fujikura Ltd., Sakura, Chiba 285-8550 Japan.

R. Yoshida, T. Kato, and T. Hirayama are with Japan Fine Ceramics Center, Atsuta, Nagoya 456-8587 Japan.

T. Taneda and T. Kiss are with Department of Electrical Engineering, Kyushu University, Nishi-ku, Fukuoka 819-0935 Japan.

II. Hypothesis and Objective of This Study

Interestingly, a common feature of reported examples of self-epitaxy is that substrates fabricated using IBAD were involved. Thickness dependence of $\Delta\phi$ of such examples was plotted in Fig. 1 [3], [5]-[7]. For example, CeO_2 showed self-epitaxy not only on an IBAD-GZO [3] but also on a $LaMnO_3$ (LMO)/IBAD-MgO substrate. Homo-epitaxial MgO on an IBAD-MgO substrate [5], [6] and $YBa_2Cu_3O_7$ (YBCO) on an LMO/epi-MgO/IBAD-MgO substrate [6] also showed self-epitaxy. Another example is Ge fabricated on a CeO_2/LMO/epi-MgO/IBAD-MgO substrate studied for a thin film photovoltaic cell application [7], [8]. The IBAD layer does not have to be directly beneath the layer which shows self-epitaxy.

FIG. 1 HERE

On the other hand, it is known that CeO_2 deposited on rolling-assisted-biaxially-textured substrates (RABiTS^{TM}), such as Ni and Ni-alloy tapes, does not show self-epitaxy. Since, it is conventional heteroepitaxy, $\Delta\phi$ values of both RABiTS and deposited CeO_2 become similar [3], [9]. One of the most significant differences between RABiTS and IBAD substrates is the in-plane grain size. Typical in-plane grain sizes of RABiTS and IBAD are about 50–100 μm [9], [10] and 11–25 nm [11], respectively. This implies a possibility that surface energy variations between neighboring grains in nanometer scale in an IBAD substrate may involve self-epitaxy of a material deposited on it.

We investigated a possible relationship between the crystallite size and the orientation in the IBAD layers because this could be a good candidate as one of the prerequisites for self-epitaxy. Fig. 2(a) shows a hypothetical IBAD-MgO layer. During the IBAD process, MgO particles are deposited on an amorphous substrate. At the same time, an Ar ion beam is incident on the substrate, with an angle of 45° with respect to the substrate normal, in many cases from the transverse direction of the substrate. This angle is chosen so that <100> of MgO orients to the substrate normal, longitudinal, and transverse directions. If several MgO particles form a crystallite on the substrate with a large in-plane misorientation angle ϕ with respect to the Ar ion beam direction projected in the substrate plane, the MgO particles will be ion-bombarded with a relatively high probability. However, MgO particles deposited with a small ϕ will withstand the ion-bombardment

The published version of this preprint appeared in IEEE Transactions on Applied Superconductivity 23, 6601005 (June 2013).

because an Ar ion can pass through ion channels within the MgO crystal structure without hitting any atoms/ions of the MgO crystal. MgO particles with a small ϕ will therefore nucleate and grow rapidly comparing with those with a large ϕ. Our hypothesis regarding IBAD substrates is that the smaller the misorientation angle is, the larger the sizes and the smaller the strains of the crystallites will be. The strain can be caused by the irradiation of the Ar ion beam in the forms of damages such as vacancies and/or interstitial impurity atoms. There has been a report on molecular dynamics simulations that supports this hypothesis; it suggests that the MgO crystallite growth rate is ϕ dependent since less sputtering occurs for small ϕ values [12].

FIG. 2 HERE

A crystallite with a small ϕ, according to our hypothesis, is large and has a small strain, and will attract more crystallites in subsequent deposition processes because the large size and the small strain both reduce the surface energy disadvantages. In other words, a crystallite with a small ϕ is energetically favorable. A schematic cross-section of the three layers of a CeO_2/LMO/IBAD-MgO architecture, which is a standard architecture used at ISTEC, is shown in Fig. 2(b). A thin LMO layer, of thickness 5–10 nm, is inserted between IBAD-MgO and CeO_2 layers to accommodate the lattice mismatch of the two layers. It is assumed that the LMO particles inherited the same size and strain as those of the MgO particles if the thickness of the LMO layer was less than 10 nm, because the grain size distribution on the surfaces of the MgO and LMO, measured using atomic force microscopy, were similar (up to about 15 nm). When CeO_2 is deposited on an LMO substrate, the nucleation and growth should be strongly influenced by the situation of LMO grains, especially for the surface. Large LMO grains with small strains would be more preferable for the deposited CeO_2 particles. The CeO_2 grains crystallized on the large LMO grains will eventually grow to dominant grains with small ϕ through competition with other grains with large ϕ. This is our hypothesis for roughly explaining the mechanism of self-epitaxy.

The objective of this study is to verify this hypothesis experimentally, that is, to determine whether the following relationship exists: the smaller the misorientation angle, the larger the crystallites of IBAD-MgO and LMO. In this study, we focused on the size effect rather than the strain effect, which will be the subject of future work.

III. Experimental

IBAD-MgO layers of thickness 5 nm were deposited on either ion-beam-sputtered GZO/Hastelloy^{TM} substrates or Y_2O_3/Al_2O_3/Hastelloy substrates, using an MgO target. LMO layers of thickness 5–10 nm were deposited by radio-frequency-sputtering on the IBAD-MgO layer with an LMO target. CeO_2 layers were deposited by pulsed-laser deposition (PLD). More detailed descriptions of the fabrication processes can be found elsewhere [13].

The misorientation angle dependence of crystallite size was estimated using in-plane X-ray diffraction (XRD). Three samples, whose topmost surfaces were MgO, LMO, or CeO_2, were prepared. Their thicknesses were 5, 6, and 7 nm, respectively. Their crystallite sizes were estimated from broadening of the (200) diffraction peaks of each material, using Scherrer's equation:

$$D = K\lambda / \beta \cos\theta \qquad (1)$$

D: crystallite size; K: Scherrer's constant (0.94); λ: X-ray wavelength; β: full width at half maximum of the diffraction peak in radians; and θ: incident angle of the X-ray. Note that broadening of the diffraction peaks can also be observed as a result of crystallite size distribution, inhomogeneous strains, sample size/settings, and optics used. These effects were included in the estimated crystallite sizes. To determine the misorientation angle dependence, measurements were performed with different offset angles ϕ_0, i.e., in-plane incident angles of the X-ray with respect to the sample longitudinal direction at $2\theta = 0°$. The offset angles ϕ_0 were 0, 5, 10, and 15°.

Transmission electron microscopy (TEM) was used to evaluate crystallite sizes and misorientation angles from plan-view observations. Samples were prepared by mechanical polishing with water from the Hastelloy side, with inclination angles of 2–3°. Ideally, measurements on the MgO layer were desirable, but preparation of MgO samples was very difficult because MgO samples of thickness 5 nm were damaged by mechanical polishing and water. However, LMO sample preparation was easier since LMO is relatively stable in water. Since the grain size distributions on the surfaces of MgO and LMO were similar, plan-view TEM images were observed with LMO of thickness 5 nm as a substitute for MgO.

In the plan-view TEM images, LMO grains were identified by their lattice images and the distance between fringes. Crystallite sizes were measured based on the longest diameter. Misorientation angles were measured with respect to the longitudinal/transverse direction of the sample so that the maximum angle became 45°. The measurements may contain errors in the sizes and angles because sometimes it was hard to determine the grain boundaries of neighboring grains, and also because the longitudinal/transverse directions of the samples might be slightly inclined with respect to the vertical/horizontal directions of the TEM images.

FIG. 3 HERE

FIG. 4 HERE

IV. Results and Discussion

Fig. 3 shows the offset angle ϕ_0 dependence of in-plane XRD profiles of MgO (200), LMO (200), and CeO_2 (200). Fig. 4 shows the offset angle ϕ_0 dependence of the average crystallite sizes, D_{ave}, of MgO, LMO, and CeO_2 estimated from in-plane XRD data in Fig. 3. The crystallite sizes decreased with increasing offset angle, which is equivalent to the misorientation angle. Since the estimated crystallite sizes

contain contributions from other effects such as strains, only qualitative trends could be identified rather than absolute values. It can be seen that the smaller the misorientation angle, the larger the crystallite size. The crystallite sizes of LMO and MgO were similar, which indicated that crystallites of LMO inherited the approximate sizes of the MgO crystallites. Among the three layers, the crystallite sizes of CeO_2 were the largest, which can be regarded as the beginning of self-epitaxy, even at this thickness of 7 nm.

A typical plan-view TEM image of the LMO layer is shown in Fig. 5(a). Horizontal, vertical, and normal directions of the image are approximately adjusted to longitudinal, transverse, and normal directions of the sample, respectively. Elemental analysis using energy dispersive X-ray spectroscopy indicated that most of the observed area consists of LMO; however, there is still some possibility that small amount of other phases, such as Y_2O_3, can be mixed. The LMO crystallites with diffraction from (100) are circled with dark lines. Crystallites circled with white lines indicate Y_2O_3 or LMO with diffraction from (400) or (110), respectively. Since separation of the fringes from Y_2O_3 (400) and LMO (110) are close, material of those crystallites cannot be identified from this observation. Brighter area in the upper part is the carbon protecting layer. In total, 67 LMO crystallites with diffraction from (100) were analyzed using four TEM images taken at different areas in the same sample.

FIG. 5 HERE

Fig. 5(b) shows the results for misorientation angle dependence of LMO crystallite size. The trend of the envelope in the plot shows that the smaller the misorientation angle, the larger the crystallite size. It is natural that the plot contains many points with small misorientation angle and size ranges, say within 10° and 10 nm, respectively, because the samples were polished at an oblique angle of 2–3° and the crystallites were not necessarily sliced at the largest diameter. An important feature of the plot was the envelope, which reflected the largest diameter at each misorientation angle.

These XRD and TEM results suggest that the hypothetical status of the IBAD-MgO layer, that the smaller the misorientation angle, the larger the crystallite size, is plausible. At least, the relationship in the LMO layer, which inherited that in the MgO layer, was directly verified experimentally using TEM. Such a relationship in the LMO layer would affect the self-epitaxy of the CeO_2 that is deposited directly on it.

V. Conclusions

To elucidate the mechanism of self-epitaxy of PLD-CeO_2, the in-plane misorientation angle dependence of crystallite size was investigated experimentally for IBAD-MgO and LMO layers as substrates for a CeO_2 layer. The hypothetical relationship between the substrates, i.e., that the smaller the misorientation angle, the larger the crystallite size, is plausible. This relationship is regarded as a prerequisite for self-epitaxy to occur because large crystallites with small strains would be energetically favorable when CeO_2 particles nucleate and grow on the substrate crystallites.

The relationship between the crystallite size and in-plane misorientation angle was verified experimentally by TEM observation of the LMO layers, which can be regarded as replicas of the MgO layers. The inhomogeneous strain of the crystallite could not be separated from the size effect in the XRD analysis in this study.

Future work is as follows: to separate the contribution of the strain from the size effect in the XRD analysis, to study the relationship between the crystallite size/strain of the LMO and nucleation and crystal growth of CeO_2, and to improve the self-epitaxy efficiency by controlling the parameter and optimizing the materials used.

Acknowledgment

Part of this work was supported by the New Energy and Industrial Technology Development Organization (NEDO) as a Materials and Power Application of Coated Conductors (M-PACC) Project.

References

[1] T. Muroga, T. Araki, T. Niwa, Y. Iijima, T. Saito, I. Hirabayashi, Y. Yamada, Y. Shiohara, "CeO_2 Buffer Layers Deposited by Pulsed Laser Deposition for TFA-MOD $YBa_2Cu_3O_{7-x}$ Superconducting Tape," *IEEE Trans. Appl. Supercond.*, vol. 13, pp. 2532-2534, 2003.

[2] T. Muroga, H. Iwai, Y. Yamada, T. Izumi, Y. Shiohara, Y. Iijima, T. Saito, T. Kato, Y. Sugawara, T. Hirayama, "Pulsed laser deposition method-CeO_2 buffer layer for YBCO coated conductor," *Physica C*, vol. 392-396, pp. 796-800, 2003.

[3] T. Muroga, *Smaller misorientation angle and higher throughput of self-epitaxial PLD-CeO_2 cap layer for YBCO coated conductors*, Ph.D. dissertation, Hokkaido University, Sapporo, Hokkaido, Japan, 2005, unpublished (in Japanese).

[4] T. Taneda, M. Yoshizumi, T. Takahashi, R. Kuriki, T. Shinozaki, T. Izumi, Y. Iijima, T. Saitoh, R. Yoshida, T. Kato, T. Hirayama, T. Kiss, "Grain/crystallite size dependence on self-epitaxy of buffer layer for coated conductors," *proc. 24th Intl. Cryo. Eng. Conf.-Intl. Cryo. Mater. Conf. 2012*, to be published.

[5] V. Matias, J. Hänisch, E. J. Rowley, and K. Güth, "Very fast biaxial texture evolution using high rate ion-beam-assisted deposition of MgO," *J. Mater. Res.*, vol. 24, pp. 125-129, 2009.

[6] V. Matias, B. J. Gibbons, J. Hanisch, R. J. A. Steenwelle, P. Dowden, J. Rowley, J. Y. Coulter, D. Peterson, "Experiments Using Continuous Fabrication of IBAD-MgO Based Coated Conductors," *IEEE Trans. Appl. Supercond.*, vol. 17, pp. 3263-3265, 2007.

[7] V. Selvamanickam, "Recovery Act: 'Near-Single-Crystalline Photovoltaic Thin Films on Polycrystalline, Flexible Substrates'," http://www.osti.gov/bridge/servlets/purl/993422/993422.pdf, 2010.

[8] V. Selvamanickam, S. Sambandam, A. Sundaram, S. Lee, A. Rar, X. Xiong, A. Alemu, C. Boney, A. Freundlich, "Germanium Films with Strong In-plane and Out-of-plane Texture on Flexible, Randomly Textured Metal Substrates," *J. Crystal Growth*, vol. 311, pp. 4553-4557, 2009.

[9] A. Goyal, D. P. Norton, J. D. Budai, M. Paranthaman, E. D. Specht, D. M. Kroeger, D. K. Christen, Q. He, B. Saffian, F. A. List, D. F. Lee, P. M. Martin, C. E. Klabunde, E. Hartfield, and V. K. Sikka, "High critical current density superconducting tapes by epitaxial deposition of $YBa_2Cu_3O_x$ thick films on biaxially textured metals," *Appl. Phys. Lett.* vol. 69, pp. 1795-1797, 1996.

[10] D. M. Feldmann, T. G. Holesinger, C. Cantoni, R. Feenstra, N. A. Nelson, D. C. Larbalestier, D. T. Verebelyi, X. Li, and M. Rupich, "Grain orientations and grain boundary networks of $YBa_2Cu_3O_{7-\delta}$ films deposited by metalorganic and pulsed laser deposition on biaxially textured Ni–W substrates," *J. Mater. Res.*, vol. 21, pp. 923-934, 2006.

[11] J. R. Groves, P. N. Arendt, H. Kung, S. R. Foltyn, R. F. DePaula, L. A. Emmert, and J. G. Storer, "Texture development in IBAD MgO films as

The published version of this preprint appeared in IEEE Transactions on Applied Superconductivity 23, 6601005 (June 2013).

a function of deposition thickness and rate," *IEEE Trans. Appl. Supercond.*, vol. 11, pp. 2822-2825, 2001.

[12] L. A. Zepeda-Ruiz and D. J. Srolovitz, "Effects of Ion Beams on the Early Stages of MgO Growth," *J. Appl. Phys.*, vol. 91, pp. 10169-10180, 2002.

[13] Y. Yamada, S. Miyata, M. Yoshizumi, H. Fukushima, A. Ibi, A. Kionoshita, T. Izumi, Y. Shiohara, T. Kato, T. Hirayama, "Development of Long Length IBAD-MgO and PLD Coated Conductors," *IEEE Trans. Appl. Supercond.*, vol. 19, pp. 3236-3239, 2009.

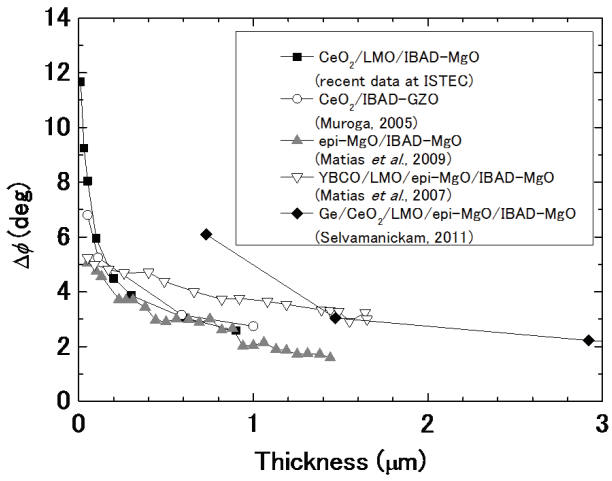

Fig. 1. Thickness dependence of in-plane misorientation angle $\Delta\phi$ of various materials that occur self-epitaxy [3], [5]-[7].

The published version of this preprint appeared in IEEE Transactions on Applied Superconductivity 23, 6601005 (June 2013).

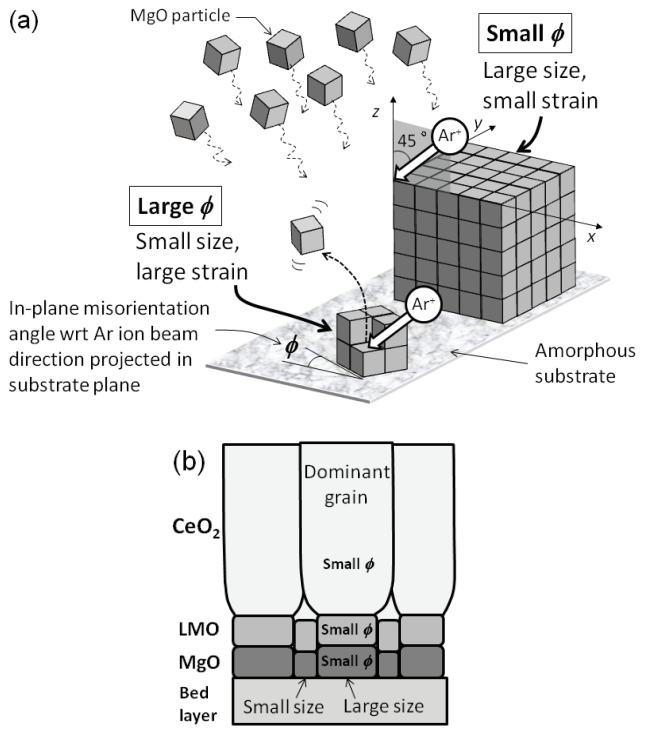

Fig. 2. (a) Hypothetical status of IBAD-MgO layer and (b) schematic cross-sections of MgO, LMO, and CeO_2 layers.

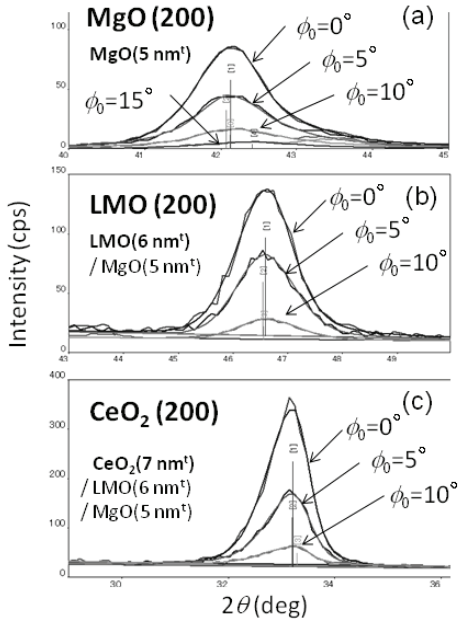

Fig. 3. Offset angle dependence of in-plane XRD profiles; sample thicknesses were 5, 6, and 7 nm for (a) MgO, (b) LMO, and (c) CeO_2, respectively.

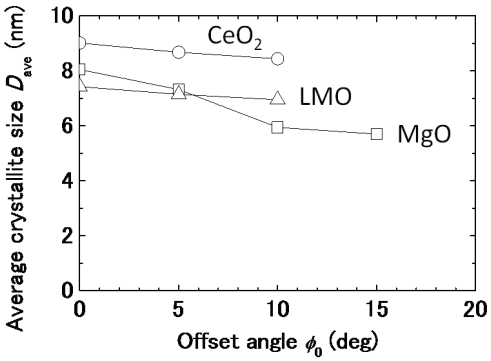

Fig. 4. Offset angle dependence of average crystallite size estimated by in-plane XRD data in Fig. 2.

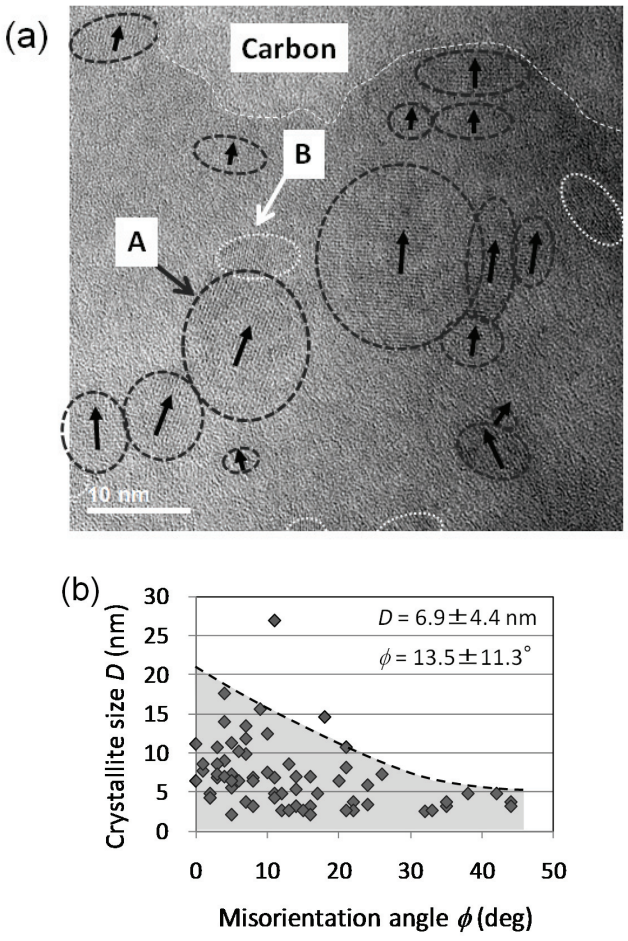

Fig. 5. (a) Typical plan-view TEM image of LMO layer of thickness 5 nm. Crystallites circled with dark lines, labeled "A," indicate LMO with diffraction from (100) while those circled with white lines, labeled "B," indicate Y_2O_3 (400) or LMO (110). (b) Misorientation angle dependence of LMO crystallite size measured from TEM images.